Product Studies of Inelastic and Reactive Collisions of NH_2 + NO: Effects of Vibrationally and Electronically Excited NH_2†

Timothy P. Marcy, Dwayne E. Heard,‡ and Stephen R. Leone*,§

JILA, National Institute of Standards and Technology and University of Colorado, and Department of Chemistry and Biochemistry, University of Colorado, Boulder, Colorado 80309-0440

Received: October 30, 2001; In Final Form: January 2, 2002

The reaction between NH_2 and NO has been studied by time-resolved step-scan Fourier transform infrared emission spectroscopy. We observe time-dependent emission from vibrationally excited NO, N_2O, and H_2O arising from the interaction of NO with both relaxed and initially vibrationally and electronically excited NH_2, produced by the 193 nm laser photolysis of ammonia. The excited NH_2 gives rise to a rapidly decaying emission signal. The correlated time dependences of the vibrationally excited NO and N_2O signals suggest that they are formed by direct collisions of NO with the vibrationally excited NH_2. There is sufficient excitation of the NH_2 to overcome the high barrier to N_2O formation. The emission from vibrationally excited H_2O shows that its formation is delayed, with a significant induction period. The time dependence of the H_2O induction period matches well to the decay of emissions from the ν_1 and ν_3 bands of NH_2, suggesting that the NH_2 is deactivated to its ground electronic and vibrational states before the water product is produced by reaction with NO.

Introduction

The reaction of NH_2 with NO has been widely studied due to its importance in the thermal De-NO_x process for reducing NO_x emission from stationary combustors.[1−13] In this process, ammonia is added to the exhaust gases of the combustor and reacts with H atoms, O atoms, or OH to produce the NH_2 that subsequently reacts with NO. This process results in a net loss of NO in the temperature range of 1100−1400 K.[1,2] Recent studies of this reaction include extensive potential energy surface and dynamics calculations and modeling of the De-NO_x process,[3−5] as well as experimental investigations probing kinetics and energetics.[1,6−10] The overall rate constant at room temperature is 1.7×10^{-11} $cm^3molecule^{-1}s^{-1}$.[3] There are three exothermic reaction channels

$$NH_2 + NO \rightarrow H_2O + N_2, \ \Delta H = -520 \text{ kJ/mol}^8 \quad (1a)$$

$$NNH + OH \rightarrow N_2 + H + OH, \ \Delta H = -27 \text{ kJ/mol}^8 \quad (1b)$$

$$N_2O + H_2, \ \Delta H = -188 \text{ kJ/mol}^4 \quad (1c)$$

for which the reaction pathways and energetics are shown in Figure 1. Reaction channel 1a proceeds through a complex series of intermediates in which all reactant bonds are broken and all product bonds are newly formed.[2−4,8] These rearrangement steps are sufficiently fast that the chemical transformation occurs without collision of the intermediate complexes under conditions relevant to the De-NO_x process.[3]

A key feature of this reaction that has not been well understood is the temperature dependence of the branching ratio between channels 1a and 1b. The fraction going to channel 1a is known to decrease with increasing temperature,[11] but the change in the 1a product fraction versus temperature has proven to be very difficult to reproduce theoretically. The calculated branching fraction depends on a number of factors including the "tightness" of several transition states in the system.[3] Recently, more detailed calculations of the NNH + OH channel have provided a much improved fit to the experimental 1a branching fraction,[5] although the theory still does not match the experimental temperature dependence completely.

Reaction 1c is expected to be unimportant in the temperature range relevant to the De-NO_x process, due to its high activation barrier of about 130 kJ/mol. The calculated rate constant for this branch at 1400 K is less than 10^{-16} $cm^3molecule^{-1}s^{-1}$.[3] Nitrous oxide that has been observed in previous experiments has been attributed to secondary reactions.[8]

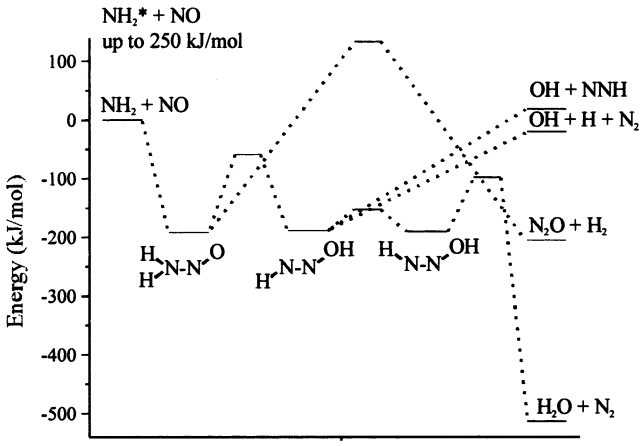

Figure 1. Proposed reaction pathways and energetics of the NH_2 + NO reactions. NH_2* produced by photolysis of ammonia in the present experiments is formed with up to 250 kJ/mol of excess energy (ref 14). Other energies in the figure are taken from refs 8 and 13.

† Part of the special issue "Donald Setser Festschrift".

‡ JILA Visiting Fellow, Permanent address: School of Chemistry, University of Leeds, Leeds, LS2 9JT, England.

§ Staff Member, Quantum Physics Division, National Institute of Standards and Technology.

10.1021/jp013997g CCC: $22.00
Published on Web 03/06/2002

In the present study, we observe infrared emission from the vibrationally excited products of the reaction of NO with NH_2 produced by 193 nm laser photolysis of ammonia. The NH_2 is formed initially with as much as 250 kJ/mol of internal energy.[14] NH_2 produced in the $\tilde{A}^2A_1$ state is almost completely collisionally quenched in our experiments in about 10 μs. We observe emission from vibrationally excited levels of NH_2 in all three normal modes of the ground $\tilde{X}^2B_1$ state. At the low total pressures used the $NH_2(\tilde{X})$ stays vibrationally excited for up to 55 μs. As we would expect, this excitation influences the reactivity of NH_2 with NO, and the lifetime of the vibrationally excited NH_2 is sufficient for the effect to be observed in our experiments. We observe the time-dependent emission from vibrationally excited H_2O, N_2O, and NO produced by this interaction and analyze the results in light of previous studies.

Experimental Section

We observe infrared emission from the vibrationally excited products of reactive and inelastic collisions between NH_2 and NO by time-resolved step-scan Fourier transform infrared (FTIR) spectroscopy.[15−18] Emission from NH_2 radicals produced vibrationally and electronically excited by the 193 nm photolysis of ammonia is also observed. Using this method, emission from many products can be probed simultaneously and the time evolution of each spectral feature can be monitored.

Because the apparatus has been discussed in detail elsewhere,[19] only a brief description is presented here. A mixture of ammonia and nitric oxide, each metered through a needle valve, is introduced into the vacuum chamber in a effusive source. Commercially available ammonia (99.99%) and NO (99%) are used without further purification. Flow rates are chosen such that the total pressure in the chamber due to the gas flow is 7 ± 1 Pa with a 3:1 ratio of NO to NH_3. The reaction region is centered between the source and sink of the gas flow, so the pressure during the reaction should be approximately the same as the measured chamber pressure. The gases are exhausted from the chamber by a 300 L/s roots blower and rotary pump combination.

The reaction is initiated by the 193 nm laser photolysis pulse creating the NH_2 radical with up to 15 000 cm^{-1} of internal energy.[14] This is sufficient to populate its electronically excited $\tilde{A}^2A_1$ state (T_0 = 11 123 cm^{-1})[20] as well as the ground $\tilde{X}^2B_1$ state. Emission from the excited NH_2 and products of the NH_2 + NO reaction are collected by Welsh cell optics and focused by CaF_2 lenses into a commercial step-scan FTIR spectrometer. In step-scan mode, the interferometer mirror is stepped through its range with a complete time history obtained at each mirror position for typically 200 co-added laser pulses. The emission is sampled in time steps of 2.5 μs and the response time of the detector and preamplifier is about 1 μs. The data thus acquired are assembled into interferograms for each time and are then Fourier transformed to give spectra at each 2.5 μs time delay.

Infrared emissions are detected with a liquid nitrogen cooled InSb detector with a lower cut off reaching 50% of maximum detectivity at 1820 cm^{-1}. For most of the experiments presented here, a 5000 cm^{-1} low pass filter is used to remove the strong emission from the electronically excited $\tilde{A}$ state of NH_2 and to allow larger steps of the moving mirror (a lower Nyquist frequency), reducing the time for data collection. Experiments were also performed with each reagent alone to help elucidate the origins of the observed emission bands. In addition, between 10 and 23 Pa of N_2 was added in an attempt to more quickly deactivate the excited NH_2 compared to deactivation of H_2O, but these experiments resulted in significant reduction in excited products observed without enough differential deactivation of the NH_2 to cause a discernible difference in the relative yields or time dependences of the products.

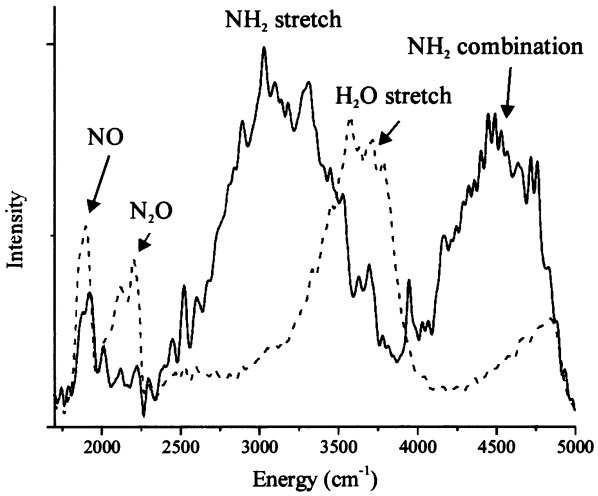

Figure 2. 20 cm^{-1} resolution emission spectra from the 193 nm photolysis of ammonia in the presence of NO obtained 10 μs (−) and 150 μs (- - -) after the photolysis pulse with the 5000 cm^{-1} low pass filter in place and a total gas pressure of 7 Pa. Relevant band origins: NO(1→0) = 1876 cm^{-1}, N_2O(100→000) = 2224 cm^{-1}, H_2O(100→000) = 3657 cm^{-1}, H_2O(001→000) = 3756 cm^{-1}, NH_2(100→000) = 3219 cm^{-1}, NH_2(001→000) = 3301 cm^{-1}.

Results

The interaction of NO with NH_2 produced by photolysis of ammonia results in infrared emission from vibrationally excited reaction products and species excited by inelastic collisions. Emission from vibrationally and electronically excited NH_2 produced by the photolysis of ammonia is also observed. The time dependences of these emissions shed light on the dynamics and kinetics of these interactions.

The presence of excited NH_2 in this process is a significant factor affecting the results. Experiments performed without the low pass filter allow the observation of the emission signal of transitions from the excited $\tilde{A}^2A_1$ state of NH_2. The rise time of this signal, integrated from 10 000 to 13 000 cm^{-1}, is limited only by the ~1 μs response time of the detection system. The time to decay to 5% of the maximum signal is about 10 μs in the typical mixture of NH_3 and NO. The emission signal from the $(v_1, v_2, v_3) \rightarrow (v_1, v_2, v_3\text{-}1)$ and $(v_1, v_2, v_3) \rightarrow (v_1\text{-}1, v_2, v_3)$ sequence bands of the $NH_2(\tilde{X})$ state, integrated from 2570 to 3120 cm^{-1}, rises to its maximum in about 10 μs. This indicates that some of the vibrationally excited ground-state radicals are the result of deactivation of the $\tilde{A}$ state. The decay of the $\tilde{X}$ state vibrational emission to 5% of its maximum is 55 μs, so the longer time behavior of the emission from products of reactive collisions with NO can be attributed to chemistry of the $\tilde{X}$ state. We believe that the $\tilde{A}$ state has less effect on the formation of the observed product species than the excited vibrational states of $NH_2(\tilde{X})$.

Figure 2 shows spectra resulting from the photolysis of ammonia in the presence of NO obtained with 20 cm^{-1} resolution and the 5000 cm^{-1} low pass filter in place. The solid line is the average of four 2.5 μs time delays between 2.5 and 10.0 μs after the photolysis pulse and the dotted line is the average of four time delays between 142.5 and 150 μs after the pulse. The early time spectrum shows strong emission from the $NH_2(\tilde{X})$ $(v_1, v_2, v_3) \rightarrow (v_1, v_2, v_3\text{-}1)$ and $(v_1, v_2, v_3) \rightarrow (v_1\text{-}1, v_2,$

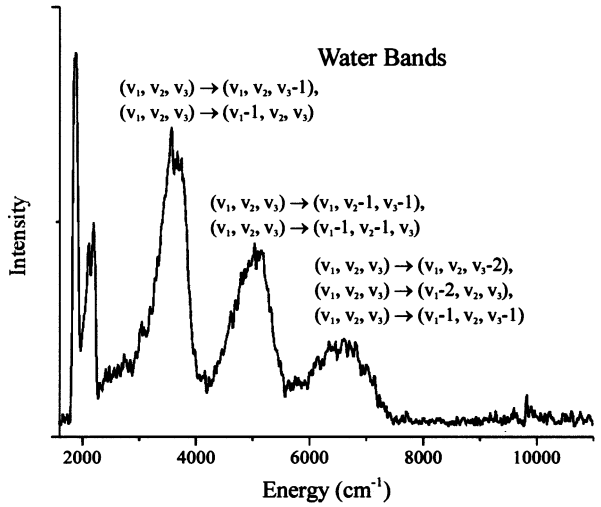

Figure 3. 20 cm^{-1} resolution emission spectrum obtained with no low pass filter 120 μs after photolysis showing the stretch fundamental, stretch−bend combination and stretch overtone of the water emission, as well as emission from NO and N_2O.

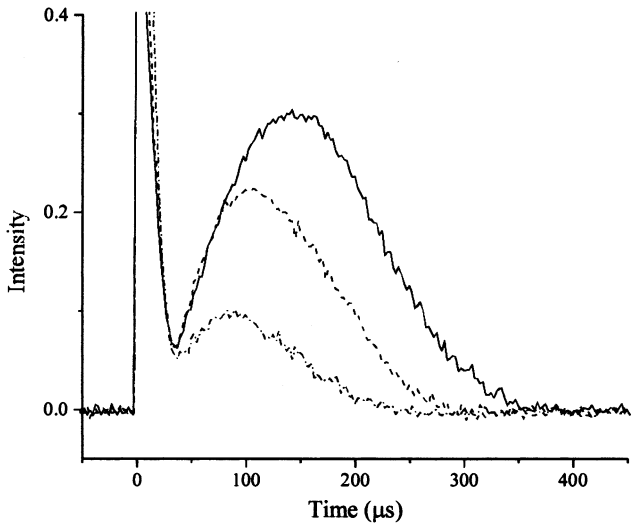

Figure 4. Time dependence of the (v_1, v_2, v_3) → (v_1, v_2, v_3-1) and (v_1, v_2, v_3) → (v_1-1, v_2, v_3) (3375−3880 cm^{-1},−), the (v_1, v_2, v_3) → (v_1, v_2-1, v_3-1) and (v_1, v_2, v_3) → (v_1-1, v_2-1, v_3) (4770−5450 cm^{-1},- - - - -), and the (v_1, v_2, v_3) → (v_1, v_2, v_3-2), (v_1, v_2, v_3) → (v_1-2, v_2, v_3) and (v_1, v_2, v_3) → (v_1-1, v_2, v_3-1) (6050−6625 cm^{-1},-·-·-) emission bands of the H_2O product.

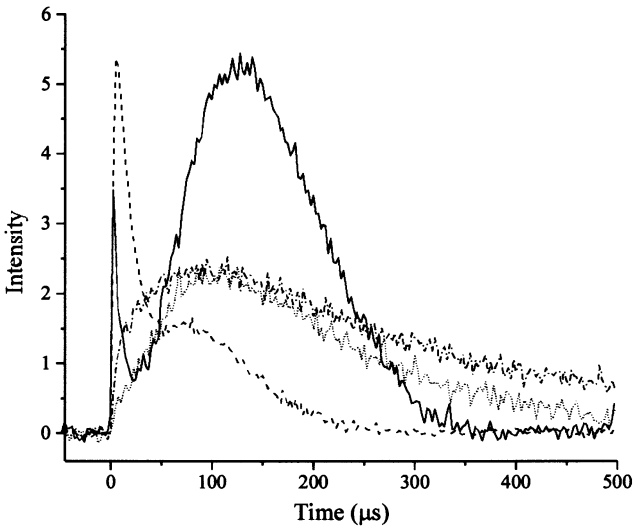

Figure 5. Time dependences of emission from H_2O (3450−3900 cm^{-1}, −), NH_2 (2750−3120 cm^{-1}, - - - - - -), NO (1830−1920 cm^{-1}, -·-·-), and N_2O (2050−21 900 cm^{-1}, ·····).

v_3) fundamental bands and the $NH_2(\tilde{X})$ (v_1, v_2, v_3) → (v_1, v_2-1, v_3-1) and (v_1, v_2, v_3) → (v_1-1, v_2-1, v_3) combination bands created directly by the photolysis of ammonia and the quenching of the $\tilde{A}$ state. These NH_2 vibrational emissions decay quickly relative to the vibrational emissions from the other molecules observed because the NH_2 $\nu_1 = 3219$ and $\nu_3 = 3301$ cm^{-1} bands are nearly resonant with the ammonia $\nu_1 = 3336$ and $\nu_3 = 3443$ cm^{-1} bands. At the later time (142.5−150 μs), the predominant emission is from the H_2O (v_1, v_2, v_3) → (v_1, v_2, v_3-1) and (v_1, v_2, v_3) → (v_1-1, v_2, v_3) bands at higher frequency. The emissions near 1900 and 2200 cm^{-1} are due to the NO(v → v-1) and N_2O (v_1, v_2, v_3) → (v_1-1, v_2, v_3) bands, respectively. We have confirmed the identity of the NO band by obtaining a spectrum with sufficient spectral resolution (0.8 cm^{-1}) to observe rotational lines and match them to known transitions in NO. We were not able to resolve individual rotational lines in the N_2O band due to a high density of states, but this emission occurs in a region of the spectrum where no other possible products of this reaction would emit. When experiments are performed without the NO, only the NH_2 emission is observed. Experiments performed with NO only do not produce any measurable signal (a noise level less than 2% of the signal with ammonia present).

Figure 3 shows the spectrum without the low pass filter, obtained 120 μs after photolysis. Three emission features containing the H_2O (v_1, v_2, v_3) → (v_1, v_2, v_3-1) and (v_1, v_2, v_3) → (v_1-1, v_2, v_3) bands, the H_2O (v_1, v_2, v_3) → (v_1, v_2-1, v_3-1) and (v_1, v_2, v_3) → (v_1-1, v_2-1, v_3) bands and the H_2O (v_1, v_2, v_3) → (v_1, v_2, v_3-2), (v_1, v_2, v_3) → (v_1-2, v_2, v_3) and (v_1, v_2, v_3) → (v_1-1, v_2, v_3-1) bands can be seen in addition to the NO and N_2O emissions. At early times, such a spectrum without the low pass filter is dominated by strong emission from the electronically excited $\tilde{A}$ state of NH_2. Figure 4 shows the time histories of integrated regions of the spectrum, each containing one of the three observed water bands. The spike at early time is due to the overlapping NH_2 emission. The times from photolysis to the maximum of the broad peak of H_2O emission are 145, 105, and 85 ± 10 μs for the (v_1, v_2, v_3) → (v_1, v_2, v_3-1) and (v_1, v_2, v_3) → (v_1-1, v_2, v_3) bands, the (v_1, v_2, v_3) → (v_1, v_2-1, v_3-1) and (v_1, v_2, v_3) → (v_1-1, v_2-1, v_3) bands, and the (v_1, v_2, v_3) → (v_1, v_2, v_3-2), (v_1, v_2, v_3) → (v_1-2, v_2, v_3) and (v_1, v_2, v_3) → (v_1-1, v_2, v_3-1) bands, respectively. The times for decay from the emission peak to 10% of the peak value are 165, 145, and 130 ± 14 μs, respectively. Both the rise and decay are slower as the energy of the transitions decreases. The deactivation of lower states is expected to be slower based on the theory of vibrational energy transfer that shows that $k_{v,v-1} \propto vk_{1,0}$, and cascading from higher vibrational levels to lower ones will slow the apparent production rate.

Figure 5 compares the time histories of the emission from the four observed species obtained with the low pass filter, which eliminates emission from the $NH_2(\tilde{A})$ state. The spectrum is integrated from 1830 to 1940 cm^{-1} for the NO emission, from 2050 to 2190 cm^{-1} for N_2O, from 2570 to 3120 cm^{-1} for the $NH_2(\tilde{X})$ (v_1, v_2, v_3) → (v_1, v_2, v_3-1) and (v_1, v_2, v_3) → (v_1-1, v_2, v_3) bands, and from 3450 to 3900 cm^{-1} for the H_2O (v_1, v_2, v_3) → (v_1, v_2, v_3-1) and (v_1, v_2, v_3) → (v_1-1, v_2, v_3) bands. The decay rate of the integrated NH_2 band is much faster than the decays of the other vibrationally excited species, but it is still eight times slower than the observed decay of the $\tilde{A}$ state. The

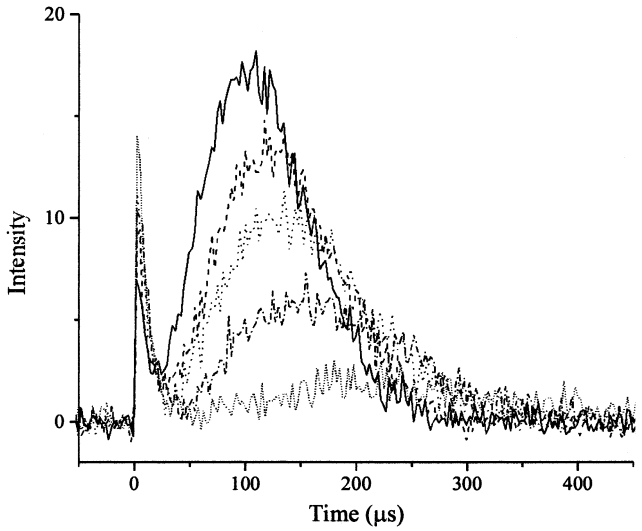

Figure 6. Time dependences of the water emission (3450−3900 cm^{-1}) with 1.6 Pa of ammonia and with 9.8 (−), 6.8 (- - -), 5.0 (· · · · ·), 3.7 (-·-·-), and 2.1 (·····) Pa of NO.

broad peak in the NH_2 trace near 90 μs is due to overlap of the water emission with this integrated band.

The NO and N_2O traces are both fairly typical of emission from species produced by direct reaction of the photolysis product. An exponential fit to the rise of the NO signal shows that it is 1.6 ± 0.1 times slower than the NH_2 (v_1, v_2, v_3) → (v_1, v_2, v_3-1) and (v_1, v_2, v_3) → (v_1-1, v_2, v_3) decay and the NO decays 10 times slower than the NH_2. The rise of the N_2O signal is even slower than the NO, likely due to significant vibrational cascading because it must be produced highly vibrationally excited because of the 130 kJ/mol barrier for this channel (see Figure 1). The observed vibrational decay time of the N_2O is much longer than the rise, so contributions from deactivation of $v_1 + 1 \rightarrow v_1$ to increasing the population in v_1 will slow the rise of the signal from that of the relatively fast reaction alone. Vibrational cascading will play a smaller role in the NO signal because it is not necessarily produced highly excited, but it is the likely cause of the rise being 1.6 times slower than the NH_2 decay. The v→v-1 transitions from the higher vibrational levels of NO (v > 2) are outside the range of the infrared detector.

The spike at early time in the H_2O emission trace is due to overlap of the 3450−3900 cm^{-1} integration window with emission from $NH_2(\tilde{X})$. The subsequent evolution of the water signal shows a distinct change of curvature during the signal rise, unlike the NO and N_2O signals, and a delay of the rise, indicating an induction period. Evidence of this induction period can also be seen in the time traces of the other vibrational transitions of water in Figure 4. The increased contribution from the overlap with $NH_2(\tilde{A})$ emission of the higher energy transitions makes a precise measurement of the induction period difficult and precludes an accurate comparison of the different vibrational levels. The presence of the induction period suggests that the observed water signal is not produced from a direct reaction of the species formed by the photolysis of ammonia. Instead, at least one of the reactants producing the vibrationally excited water must be formed by some other process, as will be discussed below, and attributed to a reaction of NO with vibrationally deactivated NH_2.

The rise and decay rates, and the amplitude of the water signal all increase as the initial amount of added NO increases while [NH_3] is held constant, as shown in Figure 6. An increase in total pressure, due to addition of NO and therefore collision frequency, will increase the deactivation rate. The overtone of the NO vibration at 3752 cm^{-1} is nearly resonant with the ν_3 fundamental of water at 3756 cm^{-1}, so the NO will likely be the primary deactivator of the water vibration. A higher NO concentration will also increase the rate of reaction. Because the rate constants for production and deactivation are similar, each process will affect both the rising and the decaying portions of the signal and yield the observed NO dependence. The change in amplitude is surprising because the NO is in considerable excess over NH_2 even at the lowest concentration used. The increase in amplitude of the signal with NO concentration implies that the rate of production of the water increases faster with [NO] than the rate of decay.

Increasing the initial concentration of ammonia, which causes an increase in initial NH_2 concentration, also results in increases in the amplitude and the rise and decay rates of the water signal. This result is expected because an increase in production rate will increase both the rising and the decaying portions of the time dependence, due to the similarity of the rates. A significant increase in the rate of production with a relatively small increase in deactivation due to the ammonia will give a greater amplitude of the water signal.

Discussion

We have seen that the 193 nm photolysis of ammonia in the presence of nitric oxide gives rise to infrared emission from electronically and vibrationally excited NH_2 produced by the photolysis as well as from vibrationally excited H_2O, N_2O, and NO. The decay of the electronically excited NH_2 occurs before the reactions proceed to a significant extent, whereas its ground state vibrational decay is slow enough to observe effects on the subsequent reactions and products. In particular, we will show that the vibrationally excited NH_2 must relax significantly before the H_2O product can be formed. This may be expected because the reaction must pass through the series of intermediates shown in Figure 1 to produce the water product. The excitation of the NH_2 reactant also allows the formation of the vibrationally excited N_2O product and vibrationally excited NO from energy transfer.

The excited N_2O and NO have not been observed in previous studies. The time dependence of the rise of the respective signals suggests that they are directly produced by the excited-state NH_2 + NO reaction or inelastic collisions. There is sufficient energy available in the excited NH_2 (250 kJ/mol) to give up to v = 4 in NO by direct energy transfer, which is the most likely mechanism producing the observed NO(v). The observed NO signal is primarily due to the v = 1→0 transition because the cutoff wavelength of the detector does not allow the observation of vibrational levels higher than v = 2. The 0.8 cm^{-1} resolution spectrum of NO does show several v = 2→1 lines. Any emission from the v = 2→0 overtone of NO at 3752 cm^{-1} would be buried in the water emission band. The rate of production of NO is 1.6 times slower than the decay of the excited NH_2. This slowing of the rise is most likely due to vibrational cascading from higher levels in the NO.

There is also sufficient energy in the excited NH_2 to overcome the 130 kJ/mol barrier to formation of $N_2O + H_2$. The N_2O is expected to be produced highly excited via reaction 1(c). The barrier to reaction plus the exothermicity of the reaction to form $N_2O + H_2$ imparts a total of 318 kJ/mol, or 26 600 cm^{-1} to the products, sufficient to populate up to $v_1 = 12$ in N_2O, calculated using the reported[21] frequency and anharmonicity of N_2O. The slower rise of the N_2O signal compared to the NO signal in Figure 5 is most likely due to the greater degree of cascading through more vibrational levels.

In contrast to the emissions from the directly produced N_2O and NO, the production of H_2O is delayed and the observed time profile has a sigmoidal shape. This strongly suggests an induction period in addition to the reactive rise of the signal and that the observed excited water is not directly produced. Water is expected to be a primary product of the reaction of NH_2 with NO, even though this requires a process in which all bonds in the reactants are broken.[3,4,8] The presence of the excited N_2O product and NO from energy transfer are a confirmation of the known[11] shift in branching fraction away from H_2O at high temperatures, but this alone does not explain the observed induction period of the water signal. The barrierless association of the reactants to form the initial complex is the rate-limiting step,[3] and therefore, this association should not result in an observed induction period.

We now consider several other possible mechanisms to account for the induction period, concluding that the difference in reactivity of NO with NH_2 with and without vibrational excitation is the most likely cause. The induction period could be an indication that the water molecules that produce the observed signal are products of a secondary reaction. However, the only other primary channel (1b) that is expected to be significant produces OH, which could form H_2O by subsequently recombining with H atoms produced by the photolysis of ammonia, or by reacting with the ammonia itself. The low density of OH and H radicals and low total pressure makes recombination highly unlikely. The exothermicity of the NH_3 + OH reaction is only 3300 cm^{-1}, which is not enough to excite even one quantum of stretching vibration in the water product. Absorption of 193 nm photons by ammonia results in almost unit yield of the NH_2 + H products,[22] so there should be little or no excited ammonia to provide more energy to the products of the NH_3 + OH reaction. In addition, neither of these possibilities explain the absence of the direct H_2O producing channel that has been universally observed or predicted by previous studies.[1−13]

Another possible explanation for the H_2O induction period could be vibrational cascading in the water from highly excited levels produced by the exothermic reaction to the lower levels. Vibrational levels up to v_1 or v_3 = 12 are within the 520 kJ/mol exothermicity of the reaction without including additional energy that may come from excited NH_2. If there is significant cascading, and if the lower vibrational levels of H_2O, from which emission is observed, are not populated directly by the reaction, then cascading from the higher levels that are created directly could lead to an induction period. This can be modeled with the simplified reaction sequence

$$NH_2 + NO \rightarrow H_2O(v_3 > 1) + N_2 \quad (2)$$

$$H_2O(v_3 > 1) + M \rightarrow H_2O(v_3 = 1) + M \quad (3)$$

$$H_2O(v_3 = 1) + M \rightarrow H_2O + M \quad (4)$$

where M is most likely NO, due to the near resonance of the NO overtone with the ν_3 mode of water. An equivalent scheme would apply to ν_1, as well, or some combination of the two modes. The $H_2O(v_3 = 1)$ signal will rise more slowly than the $H_2O(v_3 > 1)$ signal because it depends on both the production and the subsequent deactivation of $H_2O(v_3 > 1)$. A sufficient number of steps in such a cascading process could produce an effect in the $H_2O(v_3 = 1)$ population like the observed induction period. However, the highest vibrational levels of the water will be produced solely by the reaction and will not be subject to this effect. If we can observe that the highest levels also have an induction period and are not produced significantly faster than the lower levels, then vibrational cascading cannot explain the induction period. The 3450−3900 cm^{-1} region integrated for the water band time dependence in Figure 5 contains emission from several vibrational levels, and there is evidence for water emission down to about 2400 cm^{-1}. This low energy emission at later times does not come from NH_2 because its production requires NO; it does not appear when only ammonia is photolyzed.

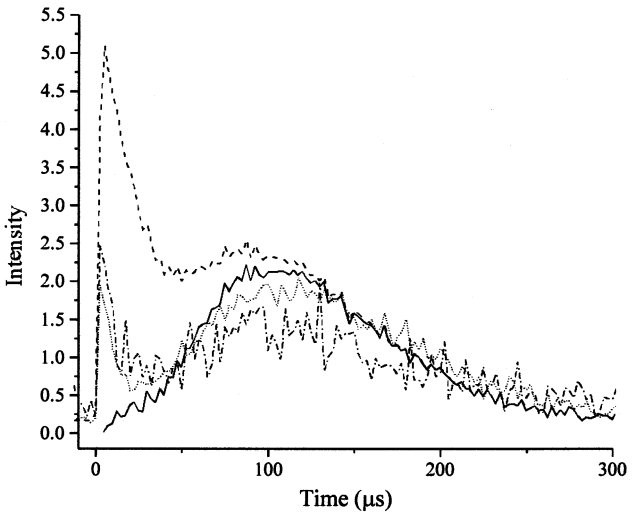

Figure 7. Time dependences of emission bands integrated from 2360 to 2420 cm^{-1} (-·-·-, multiplied by two for clarity), 3175−3390 cm^{-1} (- - -), and 3850−3950 cm^{-1} (·····), and signal resulting from the subtraction of the NH_2 contribution from the 3175−3390 cm^{-1} data (−).

Figure 7 shows the time dependence of three narrow integrated regions of the spectrum: 2360−2420 cm^{-1}, 3175−3390 cm^{-1}, and 3850−3950 cm^{-1}. We will analyze these regions to determine if there is a similar induction period for the higher and lower states. The highest energy region should contain almost exclusively emission from the (001) → (000) transition of water (and some NH_2 emission at early time). The lower energy regions will contain emission from excited vibrational states. The maximum energetically accessible stretching levels of water without including energy from excited NH_2 are v_1 or v_3 =12. The off diagonal anharmonicities for H_2O are small enough that the most anharmonically shifted emission bands will be the (12,0,0) → (11,0,0) and (0,0,12) → (0,0,11) transitions, with origins at 2686 and 2700 cm^{-1}, respectively, based on published constants.[21] The emission from water in the 2360−2420 cm^{-1} region cannot then come from stretching transitions. The (020) → (000) bending overtone of H_2O has its origin at 3151 cm^{-1}, and anharmonically shifted (v_1,v_2,v_3) → (v_1,v_2-2,v_3) bands that are well within the available energy can appear as low as 2400 cm^{-1}. We know that there is bending excitation in the water because a stretch−bend combination band appears near 5000 cm^{-1} in the spectrum in Figure 3. The 2360−2420 cm^{-1} region in Figure 7 will contain only emission from the bending overtone sequence bands (and some NH_2 emission at early time).

The 3175−3390 cm^{-1} region lies just above the bending fundamental and will contain emission from some of the most highly excited stretching levels that do not overlap with the bending overtone emission. This region of the spectrum should have the least possible effect from vibrational cascading, while the 3850−3950 cm^{-1} region will have the most. It appears that both of these regions have induction periods, but since there is

more emission from NH_2 in the 3175−3390 cm^{-1} region, it is useful to subtract the NH_2 contribution to more clearly see the time behavior of the water emission. The subtraction is accomplished by fitting a single exponential decay to the early part of the NH_2 decay curve and subtracting the fitted exponential from the data. The result is the solid line in Figure 7. The ν_1 and ν_3 stretches of H_2O will equilibrate at a rate that is near gas kinetic,[23] so by the time the water emission is observable there will not be any emission from states that are highly excited in only one of these two modes. The maximum of the water signal occurs at nearly the same time for all three integration regions. There is a distinct change of curvature and an induction period in the 3175−3390 cm^{-1} trace with the NH_2 contribution subtracted. Both the rise and the decay of this signal are slightly faster than for the 3850−3950 cm^{-1} region. This is expected because the production of water in the lowest vibrational levels is slowed by vibrational cascading, and because the rates of production and deactivation are similar. There appears to be a similar induction period for the 2360−2420 cm^{-1} region time trace, although the low signal-to-noise prohibits a more quantitative treatment. The overall similarity and the presence of the induction period in all three time traces suggest that the induction period is not due exclusively to vibrational cascading.

An explanation for the water induction period becomes clearer when we consider that NH_2 is produced by 193 nm photolysis, which yields vibrationally and electronically excited NH_2. What is unique to this investigation is that the total pressure in the reaction region is low enough that the vibrationally excited species survive for a measurable time period and the time history of the vibrational emission provides a unique clock for monitoring the formation and decay of various species. A comparison of the rates of production and decay of the observed species can elucidate the processes occurring. The decay time of the emission from the NH_2 $(v_1, v_2, v_3) \rightarrow (v_1, v_2, v_3\text{-}1)$ and $(v_1, v_2, v_3) \rightarrow (v_1\text{-}1, v_2, v_3)$ sequence bands seen in Figure 5 appears to be similar to the induction component of the water signal, excluding the reaction contribution. We can rule out any significant effect of the decay of the NH_2 $\tilde{A}$ state, which has also been observed under the conditions of these experiments to be much faster than the $\tilde{X}$ state vibrational deactivation, being depleted to 5% of its maximum within about 10 μs. Thus, the electronically excited $\tilde{A}$ state is depleted before a significant amount of reaction producing water takes place and does not likely contribute to the induction period of the water signal. To directly compare the water induction period and the $NH_2(\tilde{X})$ vibrational decay, we subtract the H_2O signal from the 2570−3120 cm^{-1} trace, leaving only NH_2 signal and fit this signal to an exponential decay in Figure 8a. The 1/e time constant of the fit is 18 ± 1 μs. We then subtract the contaminating NH_2 signal from the 3450−3900 cm^{-1} integrated region time trace, leaving only the H_2O signal in Figure 8b. The induction portion of the curve is fit with an exponential of time constant 20 ± 3 μs. The later part of the water signal rise is affected by the vibrational deactivation, which has a similar rate constant to the reaction, in addition to the reactive production and vibrational cascading of $H_2O(v)$. Fitting the entire water signal rise would require multiple exponentials, and the number of parameters would preclude accurate determination of any individual component of the fit. The similarity of the decay time for the NH_2 to relax to its ground electronic and vibrational state and the induction period of the water suggests that only vibrationally and electronically relaxed NH_2 can react with NO to yield the H_2O product.

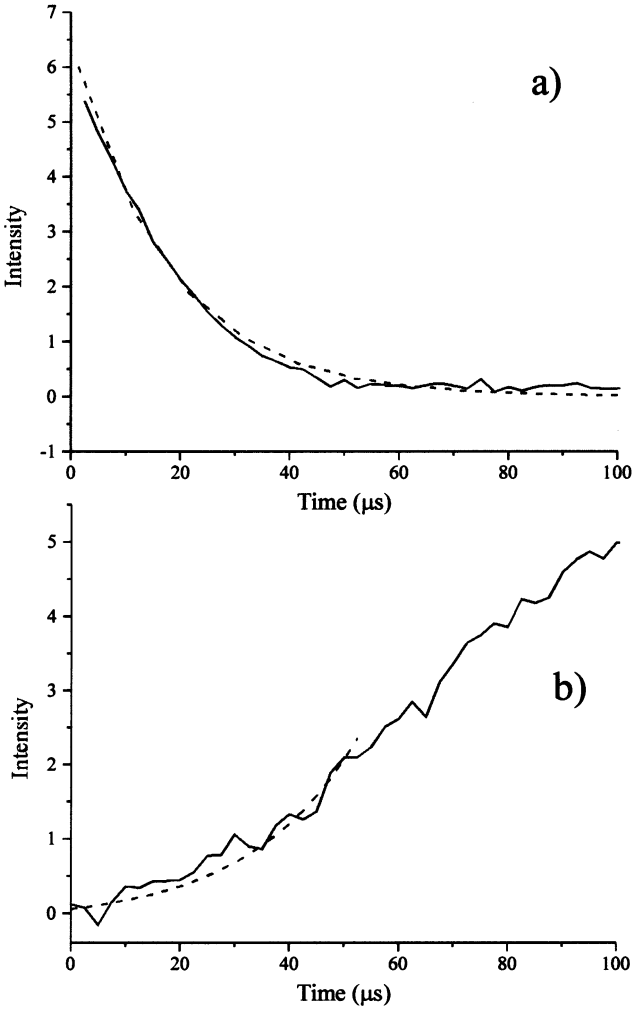

Figure 8. (a) The NH_2 signal decay (2750−3120 cm^{-1}) with the H_2O contribution subtracted for clarity (−) and an exponential with a 1/e time constant of 18 ± 1 μs (- - -). (b) The water signal rise (3450−3900 cm^{-1}) with the NH_2 contribution subtracted (−) and an exponential fit to the induction portion with a 1/e time constant of 20 ± 3 μs (- - -).

The necessary deactivation of NH_2 for the reaction to produce water can be expected because a large fraction of any intermediate complex formed from NO and excited NH_2 would return to reactants quickly, due to the excess energy present in the system. Progressing through the series of intermediates (see Figure 1) to the water product with this excess energy, without dissociation before the rearrangement is complete, would be very unlikely. None of the previously reported experimental work involved such a highly excited NH_2 reactant. Some of this excess NH_2 energy is most certainly transferred to the NO during collisions and gives rise to the observed signal from vibrationally excited NO. In addition, the excess energy of the NH_2 is sufficient to overcome the barrier to formation of N_2O, enabling the observation of that product in highly vibrationally excited states.

The case for vibrational relaxation of the NH_2 as the source of the H_2O induction is also consistent with the observed NO dependence of the amplitude and the temporal behavior of the water emission signal shown in Figure 6. If water is a primary product of the initially excited NH_2 and NO and NO is primarily responsible for the deactivation of H_2O, then the peak of the water signal should occur when

$$\frac{d[H_2O]}{dt} = k_{rxn}[NH_2][NO] - k_{deact}[H_2O(v)][NO] = 0 \quad (5)$$

where k_{rxn} is the rate constant for the production of water and k_{deact} is the rate constant for collisional deactivation. The rate constant for vibrational deactivation of H_2O by NO has been measured to be $(2.5 \pm 1.3) \times 10^{-11}$ $cm^3molecule^{-1}s^{-1}$,[12] which is the same within the error bars as the rate constant for the NH_2 + NO reaction. The increases in the rates of rise and decay should both be linear with NO concentration, so there should be no effect on the amplitude, and there must be an additional increase in the production rate to cause the observed increase in amplitude. Either the concentration of NH_2 is affected by a change of initial NO concentration, or there are additional factors governing the water production rate that are not taken into account by eq 5. If the NH_2 must first be vibrationally relaxed to produce water, then the increase in pressure will increase the NH_2 relaxation rate, which will both shorten the induction period of the water and further increase its rate of production and thus the amplitude will increase, which is what is observed.

It is highly unlikely that the observed H_2O is a secondary product of a radical−radical interaction rather than the expected product of NH_2 + NO. The emission bands that we observe and their time dependences, including the induction period of the H_2O trace, are consistent with the idea that hot NH_2 interacting with NO produces vibrationally excited NO (via inelastic collisions) and N_2O (via reactive collisions), but cannot proceed through the necessary series of intermediates to produce H_2O. Once the NH_2 relaxes to its ground electronic and vibrational states, water is formed as a product of reaction with NO. These results are in agreement with the known reduction in branching to the water product with increasing temperature. Furthermore, this process may be an additional factor, not previously accounted for in the models, contributing to the unusual change of curvature of the function of branching to the water channel with temperature.

Acknowledgment. This work was supported by the U. S. Department of Energy, Office of Basic Energy Sciences. In addition, we gratefully acknowledge additional equipment provided by the National Science Foundation. D.E.H. is grateful to JILA for the award of a Visiting Fellowship.

References and Notes

(1) Votsmeier, M.; Song, S.; Hanson, R. K.; Bowman, C. T. *J. Phys. Chem. A.* **1999**, *103*, 1566.
(2) Miller, J. A.; Bowman, C. T. *Prog. Energy Combust. Sci.* **1989**, *15*, 287.
(3) Miller, J. A.; Klippenstein, S. J. *J. Phys. Chem. A* **2000**, *104*, 2061.
(4) Diau, E. W.-G.; Smith, S. C. *J. Chem. Phys.* **1997**, *106*, 9236.
(5) Fang, D.-C.; Harding, L. B.; Klippenstein, S. J.; Miller, J. A. *Faraday Discuss.* **2001**, *119*, in press.
(6) Park, J.; Lin, M. C. *J. Phys. Chem. A* **1999**, *103*, 8906.
(7) Glarborg, P.; Kristensen, Per G.; Dam-Johansen, K.; Miller, J. A. *J. Phys. Chem. A* **1997**, *101*, 3741.
(8) Wolf, M.; Young, D. L.; Durant, J. L. *J. Phys. Chem. A* **1997**, *101*, 6243.
(9) Atakan, B.; Jacobs, A.; Wahl, M.; Weller, R.; Wolfrum, J. *Chem. Phys. Lett.* **1998**, *155*, 609.
(10) Stephens, J. W.; Morter, C. L.; Farhat, S. K.; Glass, G. P.; Curl, R. F. *J. Phys. Chem.* **1993**, *97*, 8944.
(11) Diau, E. W.; Yu, T.; Wagner, M. A. G.; Lin, M. C. *J. Phys. Chem.* **1994**, *98*, 4034.
(12) Dreier, T.; Wolfrum, J. *Twentieth Symposium (International) on Combustion;* The Combustion Institute, 1984; p 695.
(13) Melius, C. F.; Binkley, J. S. *Twentieth Symposium (International) on Combustion;* The Combustion Institute, 1984; p 575.
(14) Koplitz, B.; Xu, Z.; Wittig, C. *Chem. Phys. Lett.* **1987**, *137*, 505.
(15) Leone, S. R. *Acc. Chem. Res.* **1989**, *22*, 139.
(16) Rogers, S. A.; Leone, S. R. *Appl. Spectrosc.* **1993**, *47*, 1430.
(17) Sloan, J. J. *Advances in Spectroscopy*; Wiley: New York, 1989; Vol. 18.
(18) Hancock, G.; Heard, D. E. In *Advances in Photochemistry*; Volman, D. H., Hammond, G. S., Neckers, D. C., Eds.; Wiley: New York, 1993; Vol. 18, pp 1−65.
(19) Reid, J. P.; Qian, C. X. W.; Leone, S. R. *Phys. Chem. Chem. Phys.* **2000**, *4*, 853.
(20) Jacox, M. E. *Vibrational and Electronic Energy Levels of Polyatomic Transient Molecules;* NIST: Gaithersburg, MD, 1994.
(21) Herzberg, G. In *Infrared and Raman Spectra of Polyatomic Molecules;* Van Nostrand: Princeton, NJ, 1945.
(22) Donnelly, V. M.; Baronavski, A. P.; McDonald, J. R. *Chem. Phys.* **1979**, *43*, 271.
(23) Zittel, P. F.; Masturzo, D. E. *J. Chem. Phys.* **1991**, *95*, 8005.
(24) Vervloet, M. *Mol. Phys.* **1988**, *63*, 433.